JOURNAL OF SOLID STATE CHEMISTRY 90, 216–227 (1991)

The Defect Solid Solution $Na_{7/8}(Fe^{III}_{7/8+x}Ti^{IV}_{9/8-2x}Sb^{V}_{x})O_4$ ($0 \leq x \leq 1/3$): Evidence of Na^{I} Mobility in the Tunnels of a Quadruple Rutile-Chain Structure

F. ARCHAIMBAULT AND J. CHOISNET

Laboratoire de Cristallochimie et Réactivité des Matériaux, Université d'Orléans, F45067 Orléans Cédex 2, France

Received June 22, 1990; in revised form September 7, 1990

A new defect solid solution, the series $Na_{7/8}(Fe^{III}_{7/8+x}Ti^{IV}_{9/8-2x}Sb^{V}_{x})O_4$, was synthesized. Its homogeneity range is rather wide: $0 \leq x \leq 0.33$. The incorporation of Sb^{V} gives rise to a progressive increase of the parameters of the orthorhombic unit cell. X-ray powder structure calculations point to a partial occupancy of the large double tunnels in a quadruple rutile-chain structure. A significant ordering of cations over the octahedral framework is observed, owing to a Ti^{IV}–Sb^{V} segregation. Electrical measurements emphasize a cationic conductivity, mainly related to a 1D motion of Na^{I} cations. A transition from a low activation energy process—$E_A \leq 0.20$ eV—to a high activation energy one—$E_A \approx 0.75$ eV—systematically occurs at $T \approx 440$°C, independent of the Sb^{V} concentration. A possible skew motion from a half tunnel to another one is proposed as a tentative explanation of the high-temperature conductivity mechanism.

Introduction

Recent results (*1*, *3*) concerning the crystal chemistry of the $CaFe_2O_4$ type oxides evidence two main features:

(i) A significant extent of nonstoichiometry occurs in the occupancy of the tunnels for the double rutile-chain structure of $CaFe_2O_4$; up to 30% of calcium vacancies can exist in the mixed ferrites $Ca_{1-x/2}(Fe_{2-x}S_{n_x})O_4$ (*2*).

(ii) The simultaneous presence of Sn^{IV} and Sb^{V} cations in the double rutile-chains, as observed for the solid solution $Na_2Fe_{2+x}Sn_{2-2x}Sb_xO_8$ ($0 \leq x \leq 1$) (*3*), is a supplementary proof of the easy introduction of "nd^{10}" cations in the octahedral framework of rutile like structures (*4*, *5*). In that case, a full occupancy of the tunnels is always observed.

Up to now, all the attempts to get mixed antimonates with a $CaFe_2O_4$ type defect structure, i.e., a partial occupancy of the tunnels, were unsuccessful. Keeping in mind the existence of the closely related structure of the defect ferrititanates $Na_uFe_uTi_{2-u}O_4$ obtained by Mumme and Reid (*6*), we decided to check the introduction of Sb^{V} over the octahedral framework of that quadruple rutile-chain structure. In that way, the coupled substitution $2Ti^{IV} \rightarrow Sb^{V} + Fe^{III}$ was performed in $Na_{7/8}Fe_{7/8}Ti_{9/8}O_4$.

The present results deal with the synthesis and structural characterization of a new defect solid solution: $Na_{7/8}(Fe^{III}_{7/8+x}Ti^{IV}_{9/8-2x}Sb^{V}_{x})O_4$, which exhibits both

0022-4596/91 $3.00

a partial occupancy of tunnels and the presence of a significant concentration of Sb^V in the chains ($x \leq 0.33$). We report the results of electrical measurements which point to a mobility of Na^I ions in the tunnels.

Experimental

The syntheses were performed as solid state reactions in air. Appropriate mixtures of Na_2CO_3, Fe_2O_3, TiO_2, and Sb_2O_3 were progressively heated from 600 to 925°C to ensure the decarbonation of Na_2CO_3 and, further, the full $Sb^{III} \rightarrow Sb^V$ oxidation. Several annealings at 1000°C with quenching in air and intermediate regrindings were necessary to complete the reactions. No significant weight loss was observed.

The crystallographic analysis was performed with a Guinier–Nonius camera; powder diffractograms recorded from a Philips goniometer using the Cu$K\alpha$ radiation were used for the cell parameters determinations and structure calculations.

The electron diffraction study was performed on a JEOL 120 CX electron microscope, fitted with a side-entry goniometer (±60°).

Electrical measurements were performed on cylindrical disks (ϕ = 4 mm, e = 1 mm) compacted under 300 bars and sintered at 1000°C in air. In any case, the density was better than 80% of the theoretical value. To prepare electrodes, a platinum paste was painted onto the disks faces and they were heated to 600·C. The total *ac* conductivity was obtained from a video bridge ESI (20 Hz-150 kHz). Otherwise, a polarization of electrodes was checked by a small *dc* voltage (0.5–1 V) applied to platinum electrodes expected to be blocking for sodium ions.

Results and Discussion

Using the above-described experimental method, a new solid solution was obtained. The general formula is $Na_{7/8}(Fe^{III}_{7/8+x}Ti^{IV}_{9/8-2x}Sb^{V}_{x})O_4$. It was successively proved that:

(i) The sodium amount is not variable; i.e., there is a unique composition whose most probable value is 7/8.

(ii) A significant extent of the coupled substitution $2Ti^{IV} \rightarrow Fe^{III} + Sb^V$ occurs as x reaches the largest value $x = 0.33$ ($x_{max} = 1-7/16 = 0.5625$).

Sodium Nonstoichiometry and Introduction of Sb^V

The ferrititanates $Na_uFe_uTi_{2-u}O_4$ were first (*6*) assumed to show a short range of nonstoichiometry: $0.75 \leq u \leq 0.90$. Considering the very small variation of the cell parameters of the orthorhombic cell (a = 9.255(4) Å → 9.248(4) Å; b = 11.342(4) Å → 11.344(4) Å; c = 2.970(2) Å → 2.973(2) Å for u = 0.75 and 0.90, respectively) which is nearly within the standard deviation, the occurrence of a unique composition was held to be very probable.

In fact, our own results from crystallographic analysis point to the systematic presence of some impurities on both sides of the composition u = 7/8. More precisely, an excess of $NaFeTiO_4$ ($u > 0.875$) or $Na_2FeTi_3O_8$ ($u < 0.875$) was evidenced.

In that way, the introduction of Sb^V was undertaken in the ferrititanate $Na_{7/8}(Fe_{7/8}Ti_{9/8})O_4$. Nearly 60% of the maximum theoretical amount of Sb^V was introduced in the defect ferrititanate. Beyond this limiting value, the presence of an excess of Fe_2O_3 and $NaSbO_3$ was systematically observed.

Lattice Constants

X-ray powder diffractograms were indexed in an orthorhombic cell. The parameters are close to those found for the ferrititanate (x = 0): a = 9.253(5) Å; b = 11.340(3) Å; c = 2.970(1) Å.

Figure 1 shows the variation of the cell parameters versus x. Even though the variation of a, b, and c observed for seven compositions of the solid solution is not fully

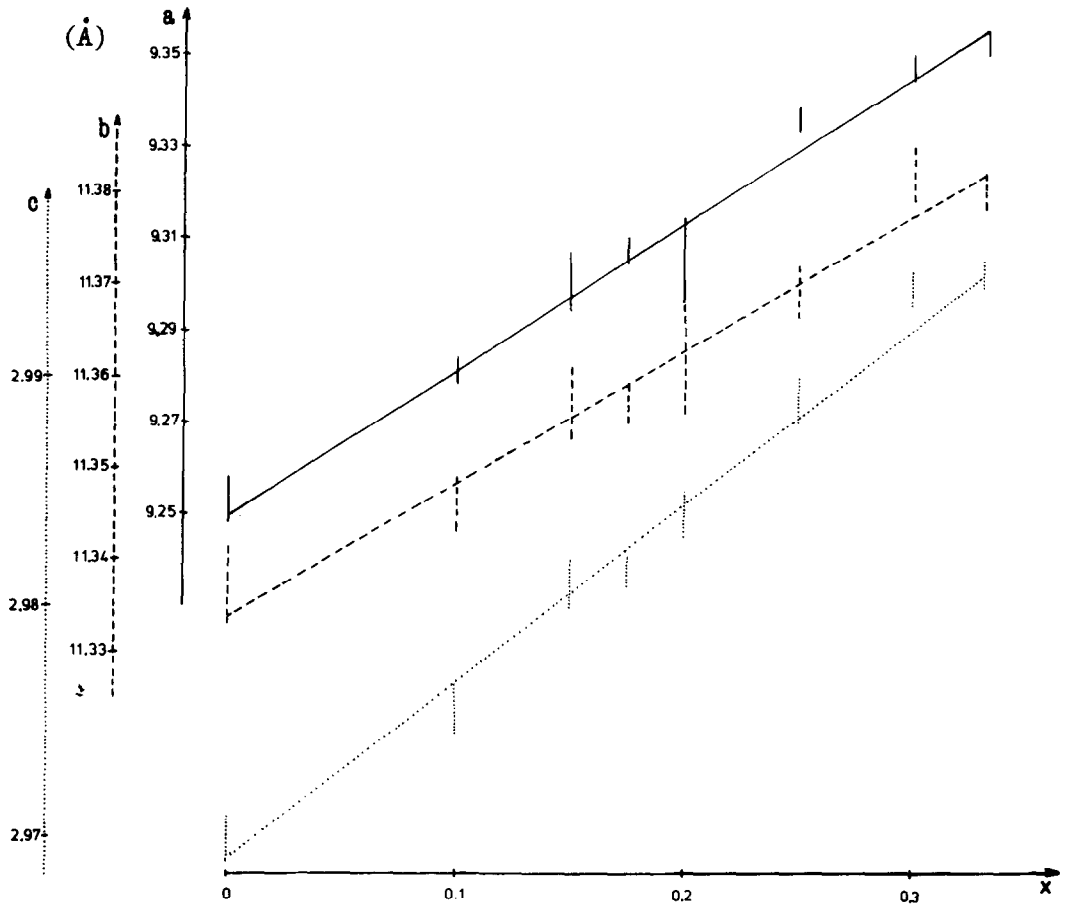

Fig. 1. Variation of the cell parameters versus x for the $Na_{7/8}(Fe_{7/8+x}Ti_{9/8-2x}Sb_x)O_4$ solid solution.

regular, it is rather well accounted for in terms of a linear law. Moreover, there is a significant increase of the cell parameters versus x which results in a larger volume of the limiting composition $V_{(x=0.33)} = 318.7(2)$ Å^3 as compared to that of the ferrititanate $V_{(x=0)} = 311.6$ Å^3. This cannot be related to the variation of ionic sizes; as a matter of fact, the mean radius in octahedral coordination calculated for $x = 0.33$, $\bar{r} = 0.63$ Å is nearly unchanged with respect to the value for $x = 0$, $\bar{r} = 0.62$ Å. In any case, this result is consistent with the comparison of the cell volumes for $NaFeTiO_4$ (*7*), $V = 291.9$ Å^3—isostructural with $CaFe_2O_4$, i.e., a double rutile-chain structure— and $Na_{7/8}(Fe_{7/8}Ti_{9/8})O_4$, i.e., the composition $x = 0$, $V = 311.6$ Å^3. In that case also, this rather large difference cannot be explained in terms of ionic sizes but probably in terms of a more open character for the quadruple rutile-chain structure of the defect ferrititanate. More generally speaking, a similar effect, i.e., the lack of a close relationship between the variation of the lattice constants and that of ionic sizes, can be observed in structures which exhibit an ionic conductivity, for example, the Nasicon type of the mixed phosphates $Na_{1+x}M^{III}_xZr_{2-x}(PO_4)_3$ (M^{III} = Cr, Ga) (*8*).

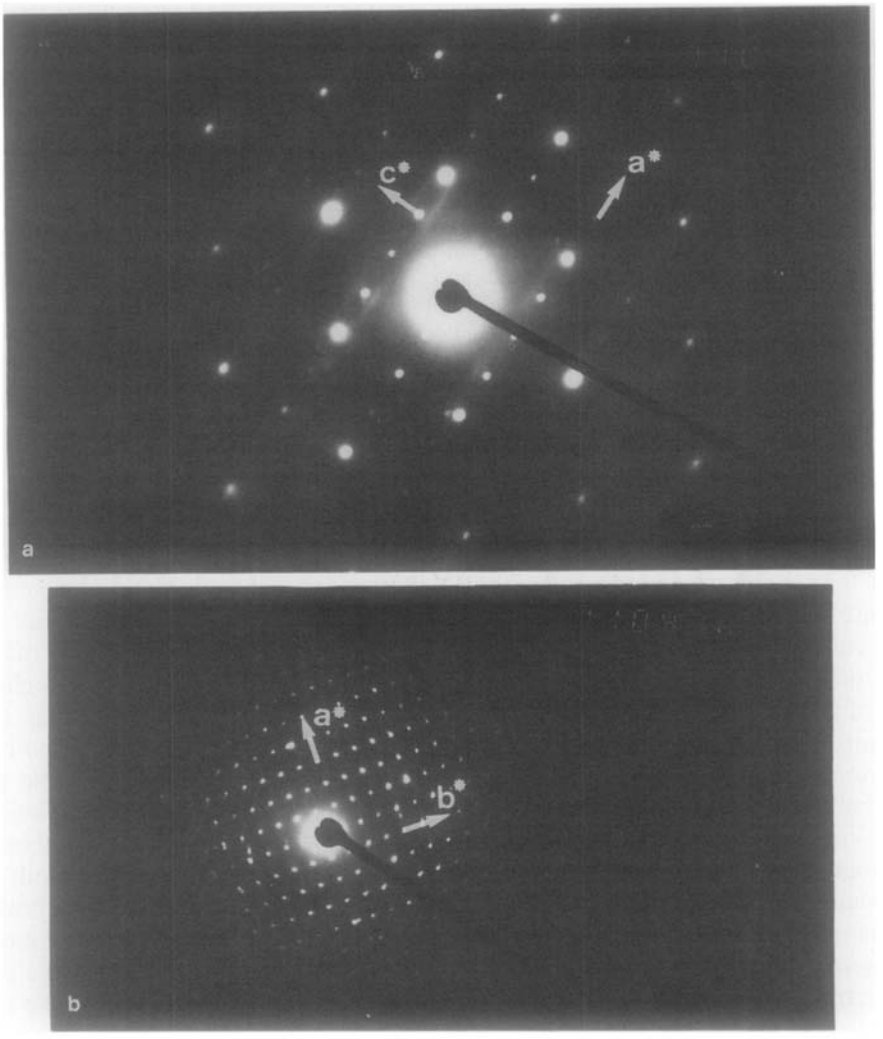

Fig. 2. Diffraction patterns of the (a) [010] plane and (b) [001] plane for $Na_{0.875}(Fe_{1.175}Ti_{0.525}Sb_{0.3})O_4$.

Structure Calculations and Crystal Chemistry

Electron diffraction study was performed on the mixed titanoantimonate $x = 0.30$. The investigation of numerous microcrystals allowed the homogeneity of the sample to be checked. The reconstruction of the reciprocal space gave evidence of an orthorhombic symmetry of the cell, with the following reflection conditions: $h0l$, $h = 2n$, and $0kl$, $k + l = 2n$, in agreement with those of the space group *Pnam* proposed for the ferrititanate $Na_{0.9}(Fe_{0.9}Ti_{1.1})O_4$ (*6*). [010] and [001] electron diffraction patterns are shown in Figs. 2a and 2b; it should be noted that $h00$ and $0k0$ reflections with $h = 2n + 1$ and $k = 2n + 1$, appearing in Fig. 2b, result from double diffraction phenomena. However, a careful examination of the electron diffraction patterns showed the ex-

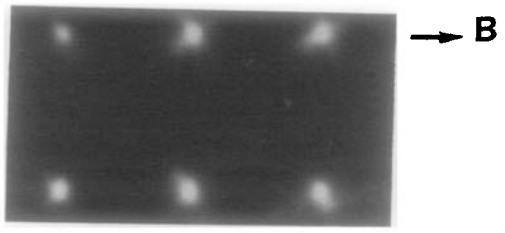

Fig. 3. Enlargement of a [001] electron diffraction pattern showing the small crosses extending along [110]* and [120]*.

istence of more complex phenomena; two types were most frequently observed:

(i) In [001] electron diffraction patterns, the diffraction spots are not circular but form small crosses extending along the [110]* and [120]* directions (Fig. 3). This suggests that the crystal had locally small distortions. In the same way, the appearance of very weak odd $h00$ spots in [010] electron diffraction patterns suggests a local loss of the symmetry (Fig. 2a).

(ii) Continuous diffuse streaks are sometimes observed along the [010]* direction in the [001] electron diffraction patterns (Fig. 4a). The corresponding bright field images show the existence of linear defects extending perpendicularly to b (Fig. 4b).

To sum up, the existence of streaks, loss of symmetry, and streaking reflections in some electron diffraction patterns suggests that short range orderings, involving small cell distortions, occur in the corresponding microcrystals; such phenomena could be related to small local variations in composition, resulting from the quenching method we used for preparing the samples.

X-ray powder structure calculations were undertaken to check the validity of the structural model $Na_{0.9}(Fe_{0.9}Ti_{1.1})O_4$ (*6*) for the defect ferriantimonate; the integrated intensities of 45 reflections (69 *hkl*) were used for a refinement procedure of atomic parameters. All the atoms occupy 4(*c*) positions: x, y, $\frac{1}{4}$ of the space group *Pnam*. As a starting point, considering a statistical distribution of Fe^{III}, Ti^{IV}, and Sb^{V} over the two sets of octahedral sites, the confidence factor $RI = \Sigma|I_0 - I_C|/\Sigma I_0$ is equal to 0.113. This first result ensures the validity of the structural model, i.e., a quadruple rutile-chain structure; still, it is not the accurate answer to the problem of the cationic distribution. As the X-ray scattering factor of Sb^{V} is much larger than those of Fe^{III} and Ti^{IV}, we decided to check the occurrence of a Ti^{IV}/Sb^{V} ordering, Fe^{III} being always statistically distributed over the two sets of octahedral sites. Table I shows the most striking results hereby evidenced: a full Ti^{IV}/Sb^{V} order is to be ruled out (RI = 0.17 or 0.45) and the best result (RI = 0.068) emphasizes a strong site preferency of Sb^{V} (80%) for the Oct(2) positions. Finally, one must keep in mind that this is a statistical result. It does not take into account some heterogeneity of the composition of microcrystals, as likely to occur from our electron diffraction study. In this

TABLE I

VARIATION OF THE CONFIDENCE FACTOR RI VERSUS THE CATIONIC DISTRIBUTION

Octahedron 1	Octahedron 2	Confidence factor	Comments
52.5%Ti + 47.5%Fe	30%Sb + 70%Fe	17%	Ti(Oct(1))/Sb(Oct(2))order
41.1% Ti + 6.5% Sb + 52.4% Fe	11.4% Ti + 23.5% Sb + 65.1% Fe	6.8%	80% site preferency Ti(Oct(1))/Sb(Oct(2)) order
30%Sb + 70%Fe	52.5%Ti + 47.5%Fe	45%	Sb(Oct(1))/Ti(Oct(2)) order

Note. □ Best value of $RI = \Sigma|I_0 - I_C|/\Sigma I_0$.

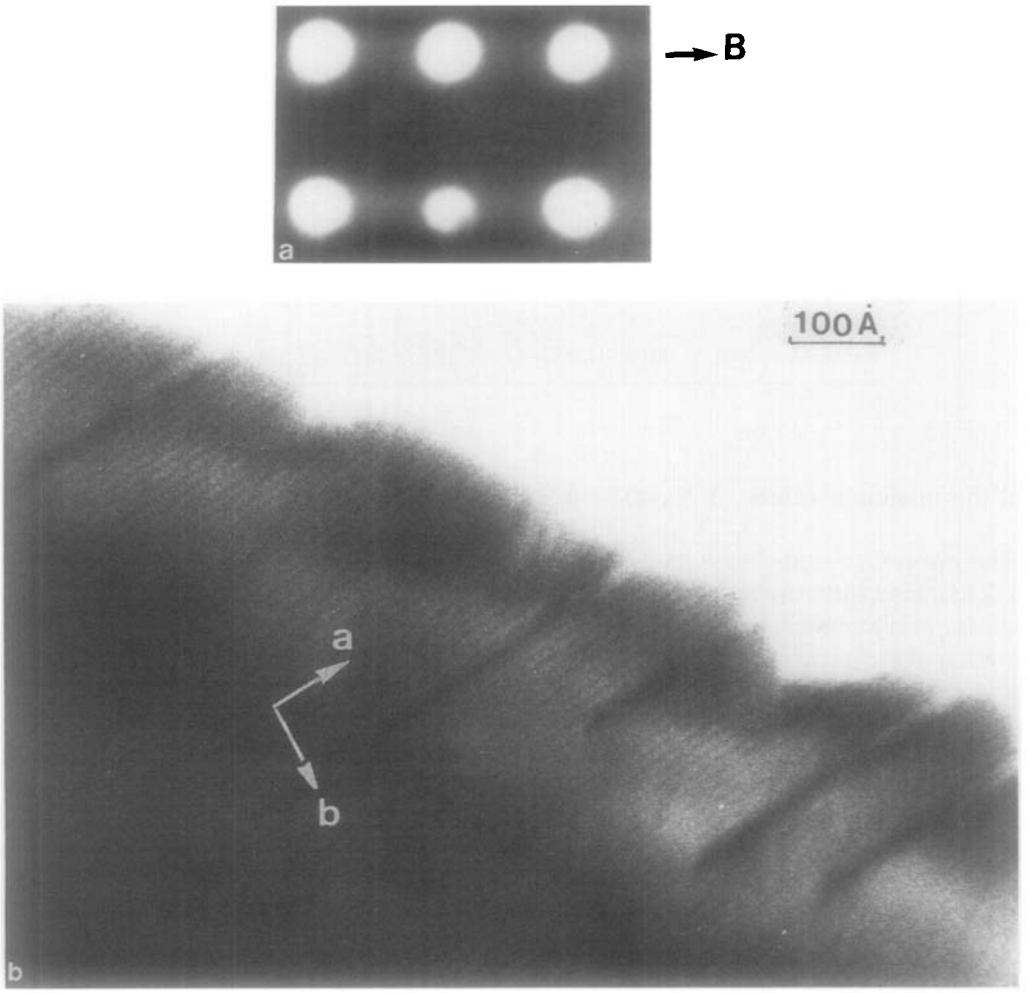

Fig. 4. (a) Enlargement of a [001] electron diffraction pattern showing weak streaks along [010]*. (b) Corresponding bright field image; linear defects are observed perpendicularly to the **b** axis.

TABLE II

ATOMIC PARAMETERS FOR $Na_{0.875}(Fe_{1.175}Ti_{0.525}Sb_{0.3})O_4$

Atoms	x	y	z	B(Å^2)
Na	0.398(3)	0.1018(1)	0.75	5.5(2)
(Fe, Ti, Sb)$_1$	0.0227(1)	0.1203(1)	0.25	0.4(1)
(Fe, Ti, Sb)$_2$	0.2341(1)	0.3406(1)	0.75	1.0(1)
O_1	0.124(2)	0.188(1)	0.75	1.1(1)
O_2	0.121(1)	0.406(2)	0.25	1.8(2)
O_3	0.355(3)	0.267(2)	0.25	3.9(1)
O_4	0.389(1)	0.460(2)	0.75	1.4(3)

way, it would be relevant to check the influence of the preparation method, for instance, annealing and slow cooling.

The final set of atomic parameters is given in Table II and the corresponding metal–oxygen distances are reported in Table III.

The mean Na–O distance, 2.50 Å, is rather consistent with the calculated value from ionic radii (2.42 Å) and thus, despite the large deviation between the maximum

TABLE III

MAIN METAL–OXYGEN DISTANCES (Å) FOR $Na_{0.875}(Fe_{1.175}Ti_{0.525}Sb_{0.3})O_4$($\Delta(M-O)$ IS THE DEVIATION BETWEEN THE MAXIMUM AND MINIMUM VALUES)

Na–O polyhedron	Octahedron 1	Octahedron 2
$O_1^{\uparrow}1 \rightarrow 2.74$	$O_1^{\uparrow}2 \rightarrow 1.934$	$O_1^{\uparrow}1 \rightarrow 2.015$
$O_2^{\downarrow}1 \rightarrow 2.24$	$O_3^{\downarrow}1 \rightarrow 2.020$	$O_2^{\downarrow}2 \rightarrow 1.976$
$O_2^{\downarrow}2 \rightarrow 2.27$	$O_4^{\downarrow}1 \rightarrow 1.993$	$O_3^{\downarrow}2 \rightarrow 2.056$
$O_3^{\downarrow}2 \rightarrow 2.44$	$O_4^{\downarrow}2 \rightarrow 2.156$	$O_4^{\downarrow}1 \rightarrow 1.994$
$\bar{d} = 2.50$	$\bar{d} = 2.032$	$\bar{d} = 2.012$
Δ (Na–O) = 0.50	$\Delta(Fe, Ti, Sb)_1$–O = 0.222	$\Delta(Fe, Ti, Sb)_2$–O = 0.08

and the minimum values, Δ Na–O = 0.50 Å.

The mean Oct–O distance shows a very weak increase with respect to the Sb^V introduction, in agreement with the very small variation of the mean ionic radius in octahedral coordination, due to the coupled substitution; $2Ti^{IV} \rightarrow Fe^{III} + Sb^V$.

The main difference is to be found in the octahedral distance deviation Δ Oct, which is significantly lowered in the Oct(2) as compared to the Oct(1). One can emphasize that a more regular character of the Oct(2) is likely to be related to the presence of a large concentration of Sb^V "d^{10}" cations.

The structure of the defect titanoantimonates $Na_{7/8}(Fe_{7/8+x}Ti_{9/8-2x}Sb_x)O_4$ is another member of the multiple rutile-chain family. The two main structural characteristics concern the octahedral framework built up from quadruple rutile-chains and the large double-"barrelled" tunnels with a partial occupancy by Na^I cations (Fig. 5). The 3D connection of quadruple rutile-chains can be described in terms of a condensation of double rutile-chains. In that way, structural relationships involving several complex oxides as $LiFeSnO_4$ (ramsdellite type) (*9*, *10*), diaspore (*11*), $CaFe_2O_4$ (*12*), and $CaTi_2O_4$ (*13*) occur. They will be investigated in a later paper.

We herein emphasize the special trend of the quadruple rutile-chain structure in the triggering of ordering phenomena when highly charged "d^{10}" cations such as Sb^V are introduced in the octahedral framework. As a matter of fact, our results concerning the titanoantimonate $Na_{0.875}(Fe_{1.175}Ti_{0.525}Sb_{0.3})O_4$ show that no more than 15% of the Sb^V in octahedral coordination is enough to observe a strong ordering phenomenon of the cationic pair (Ti^{IV}, Sb^V). Conversely, in the double rutile-chains of the $CaFe_2O_4$ type structure of $Na_2Fe_3SbO_8$ (*3*), a statistical distribution of Fe^{III} and Sb^V still remains even with 1/4 of the cations being Sb^V. In the quadruple rutile-chain structure, the existence of fully nonequivalent octahedral, Oct(1) and Oct(2), with respectively strong edge sharing and "free" O_2 vertices can be held as specially favorable to cationic ordering of the pair (Ti^{IV}, Sb^V).

The double tunnels which exist in the quadruple rutile-chain structure are not so usual in octahedral frameworks. Rutile like structures exhibit two cases, besides the defect titanoantimonate structure, as found for the psilomelane structure of $(Ba, H_2O)_2Mn_5O_{10}$ (*14*). The perspective view of the structure of $Na_{0.875}(Fe_{1.175}Ti_{0.525}Sb_{0.3})O_4$ (Fig. 6) clearly shows the two columns of Na^I cations alternately staggered in each "barrel" of the double tunnel. Owing to the

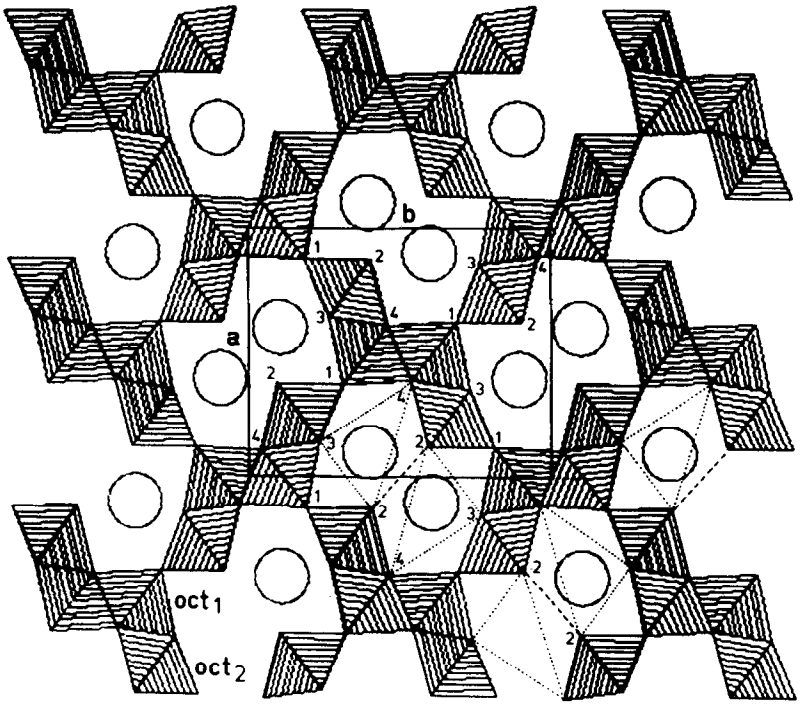

Fig. 5. Projection of the structure of $Na_{0.875}(Fe_{1/175}Ti_{0.525}Sb_{0.3})O_4$ on to the (001) plane; (----) "O_2 wall."

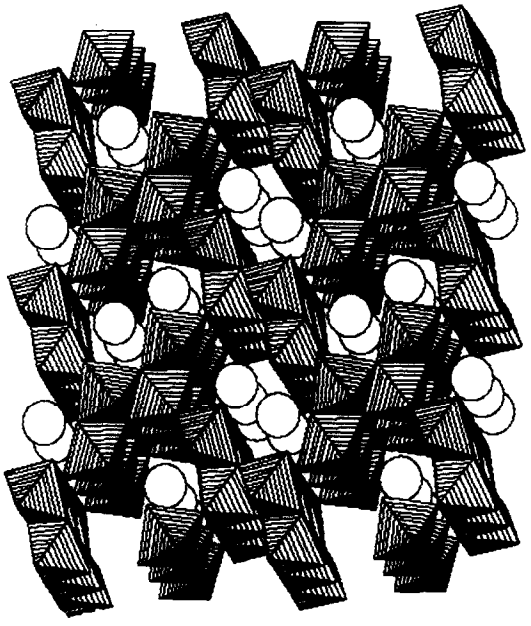

Fig. 6. Perspective view of $Na_{0.875}(Fe_{1.175}Ti_{0.525}Sb_{0.3})O_4$.

existence of some vacancies in these tunnels—12.5%—a mobility of Na^I cations is expected. The significant value of their thermal factor, $B = 5.5$ Å^2, points to such a phenomenon. Moreover, the use of an anisotropic thermal factor of Na^I in the structure calculations points to a motion mainly along the **c** axis ($U_{33} = 0.226$). Obviously, this will effect to some extent the sodium mobility in the tunnels.

Evidence of a Sodium Mobility: Electrical Measurements and a Tentative Structural Model

Electrical measurements were undertaken to check the occurrence of an ionic conductivity in the defect solid solution $Na_{7/8}(Fe_{7/8+x}Ti_{9/8-2x}Sb_x)O_4$. The ferrititanate $NaFeTiO_4$ was also considered, as it exhibits a $CaFe_2O_4$ type structure; thus, an easy comparison between the double and

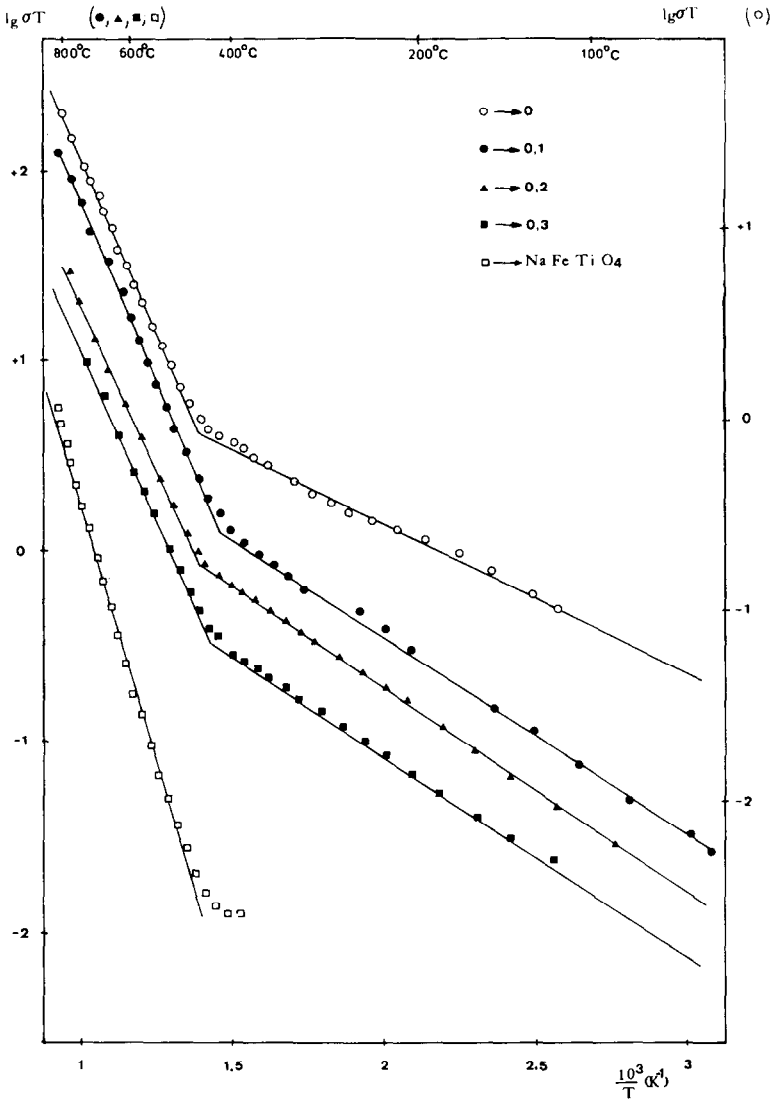

Fig. 7. Evolution of the conductivity $\log(\sigma T)$ versus $10^3/T$ for the $Na_{7/8}(Fe_{7/8+x}Ti_{9/8-2x}Sb_x)O_4$ solid solution.

the quadruple rutile-chain structures is expected. The total *ac* conductivity shows an activated behavior, as evidenced from the $\log(\sigma T) = f(10^3/T)$ plots (Fig. 7). The most striking feature is the existence of two well-defined conributions, with a transition temperature close to 440°C. In the low-temperature range (LT) (Table IV), the activation energy is rather small: $E_{A(LT)} \approx 0.20$ eV (for the Sb^V-containing composition); the lowest value of $E_{A(LT)}$ is that of the defect ferrititanate $E_{A(LT)} \approx 0.16$ eV. In the high-temperature range, $E_{A(HT)}$ is nearly constant and equal to 0.74 eV. Nevertheless, this value is smaller than that we observed for the double rutile-chain structure of $NaFeTiO_4$: $E_A \approx 1.04$ eV.

To ensure the ionic character of the con-

TABLE IV

ACTIVATION ENERGIES OF THE IONIC CONDUCTIVITY AT LOW AND HIGH TEMPERATURES FOR THE SOLID SOLUTION $Na_{7/8}(Fe_{7/8+x}Ti_{9/8-2x}Sb_x)O_4$ AND NaFeTiO$_4$

Compound	$E_{A(LT)}$(eV)	$E_{A(HT)}$(eV)
$x = 0.0$	0.16	0.74
$x = 0.1$	0.20	0.75
$x = 0.2$	0.22	0.74
$x = 0.3$	0.23	0.71
NaFeTiO$_4$		1.04

ductivity, measurements were made under a small *dc* voltage (0.5–1 V) using platinum electrodes expected to block for sodium ions. Figure 8 shows the polarization: the plots $I = f(t)$ show a time-dependent behavior at 200°C, which becomes very significant at 600°C. Therefore, an ionic conductivity is proved to exist in the two temperature ranges.

A tentative explanation of the ionic conductivity of the defect titanoantimonate can be found in the two types of ionic migration which can be considered from the above

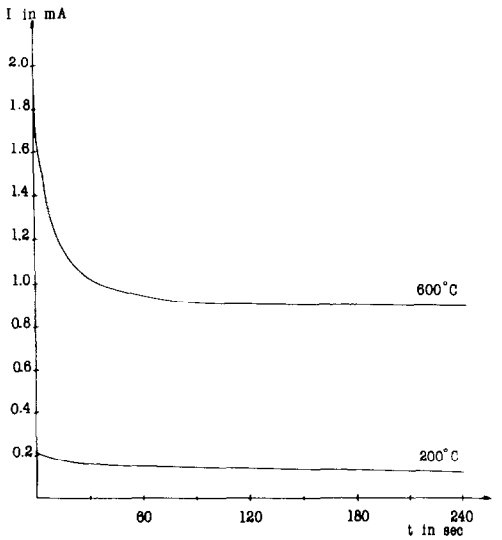

Fig. 8. Polarization tests: $I = f(t)$.

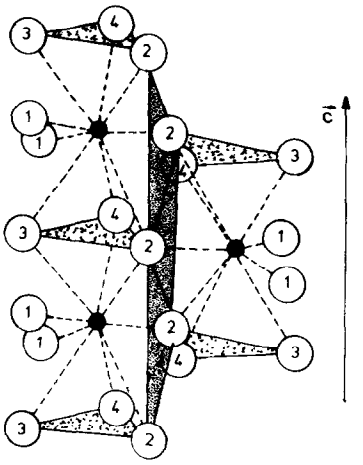

Fig. 9. Tricapped trigonal prism for $Na_{0.875}(Fe_{1.175}Ti_{0.525}Sb_{0.3})O_4$; the triangular $O_2O_3O_4$ faces are perpendicular to the *c* axis and the $O_2O_2O_2$ faces are parallel to the *c* axis. ●, Sodium; ○ oxygen.

crystal–chemical description. In fact, from one site in the double-barrelled tunnel, a Na^I cation can move toward four adjacent sites:

(i) Two sites are located in the same barrel and are reached by a 1D motion along the **c** axis, across the $O_2O_3O_4$ triangles (Figs. 5, 9, and 10a).

(ii) The two other sites are in the other barrel: they are reached by a skew motion across the "O_2 wall" built from $O_2O_2O_2$ triangles (Figs. 5, 9, and 10b).

Clearly, the axial motion is much more likely to occur than the skew motion from one barrel to the other. Crossing the $O_2O_3O_4$ triangle leads to observed Na–O distances no less than 2.50 Å (Fig. 10a), which probably means a low activation process, in agreement with the significant value of the anisotropic thermal factor of Na^I cations. Conversely, crossing the "O_2 wall" which divides the double tunnel is rather hindered by the short Na–O distance which is required: 1.95 Å (Fig. 10b). This is a typical bottle neck for ionic mobility, which looks like that existing in the Ca Fe_2O_4 type oxides (*2*). One can only sup-

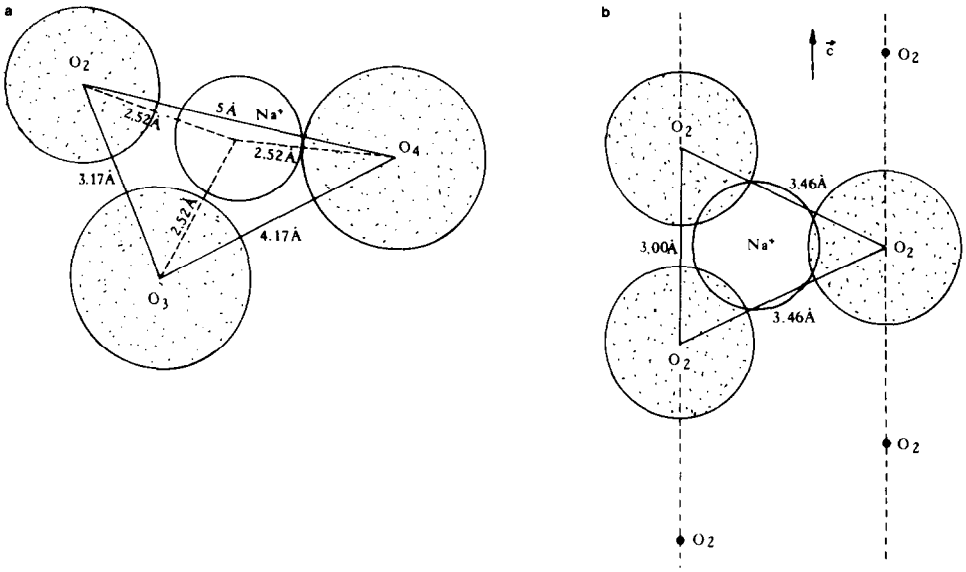

Fig. 10. (a) Oxygen triangle $O_2O_3O_4$ and (b) oxygen triangle $O_2O_2O_2$.

pose that at high temperature a shift of O_2 oxygens allows a jump between the two barrels; consequently, this will be related to a highly activated process.

Therefore, the LT ($T < 440$°C) weakly activated process would be ascribed to the axial motion in each barrel of the double tunnels while the HT ($T > 440$°C) highly activated process would be due to the skew motion of Na^I ions from one barrel to another. However, this explanation cannot be held as the true one without further information related to both electrical and structural properties. Moreover, as the transference number $t_i = \sigma_i/\sigma_t$ calculated for the LT range is significant, $t_i \approx 0.19$, the existence of two distinct migration mechanisms cannot be ensured.

Finally, a comparison with other sodium conductors or with rutile like tunnel structures leads to the following statements:

(i) The conductivity level is rather low: $\sigma \approx 10^{-4}\ (\Omega\ \text{cm})^{-1}$ at 200°C, as a consequence of the amount of vacancies not being large enough: 12.5%.

(ii) The value of the activation energy at LT, $E_A = 0.20$ eV, agrees well in a qualitative sense with the open character of the quadruple rutile-chain structure. More open tunnel structures are not so frequent: the best values of E_A recently found in rutile-like structures concern the mixed gallotitanates $A_xGa_8Ga_{8+x}Ti_{16-x}O_{56}$ (A = K, Rb, Cs) where the very large volume of the tunnels, without a bottleneck, allows an activation energy as low as 0.10 eV (*15, 16*).

Conclusion

The main features related to the defect solid solution $Na_{7/8}(Fe^{III}_{7/8+x}Ti^{IV}_{9/8-2x}Sb^{V}_{x})O_4$ are summarized below:

(i) The stabilization of a quadruple rutile-chain structure is achieved by means of the coupled substitution: $2Ti^{IV} \rightarrow Fe^{III} + Sb^{V}$.

(ii) There is a trend for a Ti^{IV}/Sb^{V} ordering in the quadruple chains.

(iii) The existence of vacancies in the double tunnels allows a sodium mobility, mainly a 1D motion as shown by the results of the electrical measurements.

The work in progress is an attempt to bet-

ter understand the conductivity–structure relationship for the quadruple rutile-chain type structure, mainly in order to improve the properties that depend on sodium mobility in the double tunnels.

Acknowledgments

We are indebted to Professor M. Hervieu, Lab. CRISMAT, Caen University (France), for the electron diffraction patterns.

References

1. F. Archaimbault, J. Choisnet, M. Hervieu, and B. Raveau, *Anna. Chim. Fr.* **12,** 23 (1987).
2. F. Archaimbault, P. Odier, and J. Choisnet, *Solid State Ionics* **28/30,** 1357 (1988).
3. F. Archaimbault, M. Rautureau, and J. Choisnet, *Europ. J. Inorg. Solid State Chem.* **25,** 1 (1988).
4. Ph. Lacorre, M. Hervieu, J. Choisnet, and B. Raveau, *J. Solid State Chem.* **51,** 44 (1984).
5. Ph. Lacorre, M. Hervieu, and B. Raveau, *Mater. Res. Bull.* **19,** 693 (1984).
6. W. G. Mumme and A. F. Reid, *Acta. Crystallogr. Sect. B* **24,** 625 (1968).
7. A. F. Reid, A. D. Wadsley, and M. J. Sienko, *Inorg. Chem.* **7,** 112 (1968).
8. J. M. Winand, A. Rulmont, and P. Tarte, *J. Mat. Sciences,* **25,** 4008 (1990).
9. A. M. Byström, *Acta. Chem. Scand.* **3,** 163 (1949).
10. J. Choisnet, M. Hervieu, B. Raveau, and P. Tarte, *J. Solid State Chem.* **40,** 344 (1981).
11. K. Sasvari and A. Zalaj, *Acta. Geol. Sci. Hung.* **4,** 415 (1957).
12. B. F. Decker and J. S. Kasper, *Acta. Crystallogr.* **10,** 332 (1957).
13. N. F. H. Bright, J. F. Rowland, and J. G. Wurm, *Canad. J. Chem.* **36,** 492 (1958).
14. A. D. Wadsley, *Acta. Crystallogr.* **6,** 433 (1953).
15. M. Watanabe, Y. Fujiki, S. Yoshikado, and T. Ohachi, *Solid State Ionics* **28/30,** 257 (1988).
16. S. Yoshikado, T. Ohachi, I. Taniguchi, W. Watanabe, Y. Fujiki, and Y. Onoda, *Solid State Ionics* **28/30,** 173 (1988).